Chinese Physics B

PAPER

Effects of chemical pressure on diluted magnetic semiconductor $(Ba,K)(Zn,Mn)_2As_2$

Effects of chemical pressure on diluted magnetic semiconductor (Ba,K)(Zn,Mn)$_2$As$_2$*

Y Peng(彭毅)[1,2], S Yu(于爽)[2,3], G Q Zhao(赵国强)[2,3], W M Li(李文敏)[2,3], J F Zhao(赵建发)[2,3], L P Cao(曹立朋)[2], X C Wang(望贤成)[2,3], Q Q Liu(刘清青)[2,3], S J Zhang(张思佳)[2,3], R Z Yu(于润泽)[2,3], Z Deng(邓正)[2,3,†], X H Zhu(朱小红)[1,‡], and C Q Jin(靳常青)[2,3,4,§]

[1] *College of Materials Science & Engineering, Sichuan University, Chengdu* 610064, *China*
[2] *Beijing National Laboratory for Condensed Matter Physics, and Institute of Physics, Chinese Academy of Sciences, Beijing* 100190, *China*
[3] *School of Physics, University of Chinese Academy of Sciences, Beijing* 100190, *China*
[4] *Collaborative Innovation Center of Quantum Matter, Beijing* 100871, *China*

(Received 2 February 2019; revised manuscript received 25 February 2019; published online 4 April 2019)

Chemical pressure induced by iso-valent doping has been widely employed to tune physical properties of materials. In this work, we report effects of chemical pressure by substitution of Sb or P into As on a recently discovered diluted magnetic semiconductor (Ba,K)(Zn,Mn)$_2$As$_2$, which has the record of reliable Curie temperature of 230 K due to independent charge and spin doping. Sb and P are substituted into As-site to produce negative and positive chemical pressures, respectively. X-ray diffraction results demonstrate the successful chemical solution of dopants. Magnetic properties of both K-under-doped and K-optimal-doped samples are effectively tuned by Sb- and P-doping. The Hall effect measurements do not show decrease in carrier concentrations upon Sb- and P-doping. Impressively, magnetoresistance is significantly improved from 7% to 27% by only 10% P-doping, successfully extending potential application of (Ba,K)(Zn,Mn)$_2$As$_2$.

Keywords: chemical pressure, (Ba,K)(Zn,Mn)$_2$As$_2$, diluted magnetic semiconductor, iso-valent doping

PACS: 75.50.Pp, 74.62.Fj, 75.50.–y **DOI:** 10.1088/1674-1056/28/5/057501

1. Introduction

A dilute magnetic semiconductor (DMS), which has potential to control charge and spin in a single material, is very applicable to spintronic devices.[1–3] Since the discoveries of (Ga,Mn)As and (In,Mn)As, the III–V based DMSs have received much attention as prototypical DMS materials.[4–6] However, in either (Ga,Mn)As or (In,Mn)As, heterovalent (Ga^{3+}, Mn^{2+}) or (In^{3+}, Mn^{2+}) substitution leads to difficulties in individual control of carrier and spin doping and seriously limited chemical solubility. These two obstacles prevent further improving the Curie temperature (T_C) of the III–V based DMS.

Recently, a series of new DMS materials with independent doping of carrier and spin have been discovered, such as Li(Zn,Mn)As and (Ba,K)(Zn,Mn)$_2$As$_2$ (BZA).[7,8] Many progresses have been made in these new DMSs on both fundamental studies and potential applications.[9–28] Among the new DMS materials, BZA has a maximum Curie temperature (T_C) of 230 K, which is a reliable record of carrier-mediated ferromagnetic DMS.[29] Large single crystals of BZA have been grown.[15] Taking advantage of single crystal-based Andreev reflection junction, the spin polarization rate of 66% is obtained for BZA, which is comparable to prototypical III–V based DMS.[15,30]

However, the lack of reliable room temperature ferromagnetism is still one of the open questions for all DMS materials. Recently, a series of studies have concentrated on physical pressure-effect on BZA to gain an insight into the mechanism of the ferromagnetism in BZA and in turn to search for a possible way to increase T_C. Although these works showed suppression of T_C with increasing external pressure, one may wonder how lattice expansion will affect the ferromagnetism in BZA. In this article, we substitute As with Sb and P to study the negative and positive chemical pressure-effect on BZA.

2. Method

Two teams of samples have been synthesized: the first is based on K-under-doped $(Ba_{0.9}K_{0.1})(Zn_{0.85}Mn_{0.15})_2(As_{1-y}Pn_y)_2$ (Pn = Sb and P; y = 0.1 and 0.2), the second is based on K-optimal-doped $(Ba_{0.7}K_{0.3})(Zn_{0.85}Mn_{0.15})_2(As_{1-y}Pn_y)_2$ (Pn = Sb and P; y = 0.1 and 0.2). The polycrystallines of all the samples were synthesized with conventional solid reaction under the protection of high-purity argon as described in Ref. [8]. Powder x-ray diffraction (PXRD) was performed

*Project supported by the National Key R&D Program of China (Grant No. 2017YFB0405703), the Ministry of Science and Technology of China (Grant Nos. 2018YFA03057001 and 2015CB921000), and the National Natural Science Foundation of China through the Research Projects (Grant Nos. 11534016 and 61504166).

†Corresponding author. E-mail: dengzheng@iphy.ac.cn
‡Corresponding author. E-mail: xhzhu@scu.edu.cn
§Corresponding author. E-mail: Jin@iphy.ac.cn

using Cu K_α radiation with a Philips X'pert diffractometer at room temperature. The DC magnetic susceptibility was characterized by a superconducting quantum interference device (SQUID) magnetometer. A physical property measurement system (PPMS) was used for electricity transport and Hall effect measurements.

3. Results and discussion

All the samples crystalize into tetrahedral $BaZn_2As_2$ phase (β-phase, space group *I*4*mmm*, as shown in Fig. 1(a)). Figure 1(b) shows the PXRD patterns of $(Ba_{0.7}K_{0.3})(Zn_{0.85}Mn_{0.15})_2(As_{1-y}Pn_y)_2$ (Pn = Sb and P; y = 0.1 and 0.2) series samples as typical examples. As expected, except some minor nonmagnetic or antiferromagnetic impurities, all the diffraction peaks move to lower degrees with higher Sb-doping level due to the larger ionic radius of Sb than As. For the same reason, P-doping moves the diffraction peaks to higher degrees. As shown in Fig. 1(b), the calculated lattice parameters further demonstrate the expansion and compression of lattice by Sb- and P-doping, respectively. The lattice parameters monotonically change with doping levels, indicating successful chemical solutions of Sb- and P-dopants.

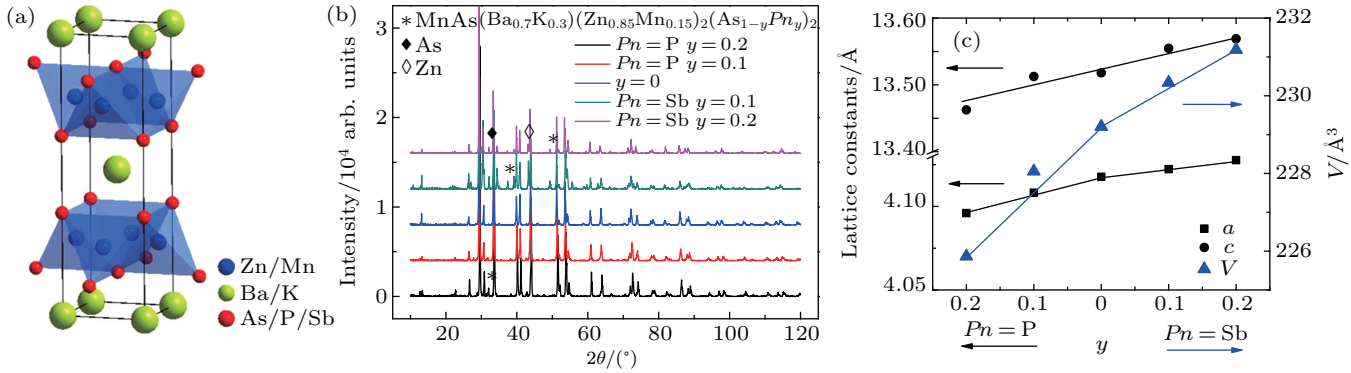

Fig. 1. (a) The crystal structure of $(Ba,K)(Zn,Mn)_2(As_{1-y}Pn_y)_2$. (b) PXRD patterns of $(Ba_{0.7}K_{0.3})(Zn_{0.85}Mn_{0.15})_2(As_{1-y}Pn_y)_2$ (Pn = Sb and P; y = 0.1 and 0.2). The mark star stands for antiferromagnetic impurity MnAs, the solid diamond for nonmagnetic As, and the open diamond for nonmagnetic Zn_3As_2. (c) Lattice constants and cell volumes of the samples in panel (b).

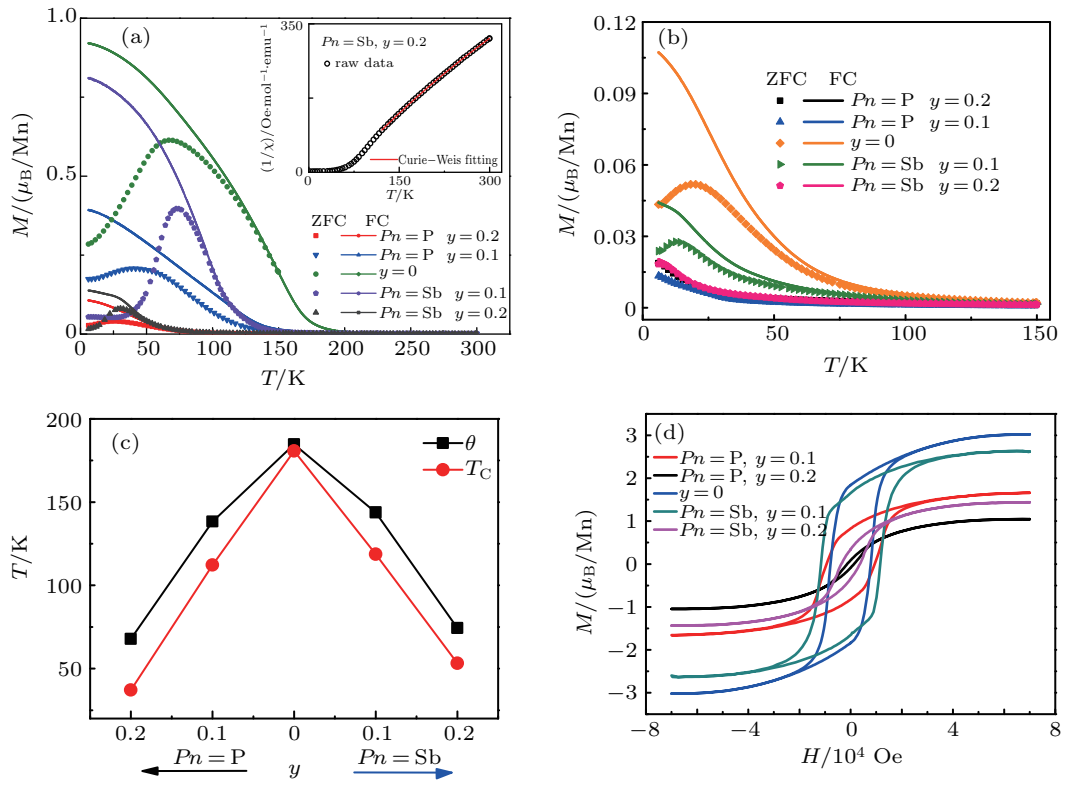

Fig. 2. The temperature dependent magnetization of (a) $(Ba_{0.7}K_{0.3})(Zn_{0.85}Mn_{0.15})_2(As_{1-y}Pn_y)_2$ (Pn = Sb and P; y = 0.1 and 0.2) and (b) $(Ba_{0.9}K_{0.1})(Zn_{0.85}Mn_{0.15})_2(As_{1-y}Pn_y)_2$ (y = 0.1 and 0.2 for Pn = Sb; y = 0.1 for Pn = P). The inset is the Curie–Weiss fit of $(Ba_{0.7}K_{0.3})(Zn_{0.85}Mn_{0.15})_2(As_{0.8}Pn_{0.2})_2$ (c) Curie temperature and paramagnetic temperature of the samples in panel (a). (d) Field dependent magnetization of the samples in panel (a) at 2 K.

Figures 2(a) and 2(b) show the DC magnetization versus temperature ($M(T)$) of $(Ba_{1-x}K_x)(Zn_{0.85}Mn_{0.15})_2(As_{1-y}Pn_y)_2$ with $x = 0.1$, 0.3; $y = 0.1$, 0.2; and Pn = Sb, P. Herein the T_C of $(Ba_{0.9}K_{0.1})(Zn_{0.85}Mn_{0.15})_2As_2$ and $(Ba_{0.7}K_{0.3})(Zn_{0.85}Mn_{0.15})_2As_2$ are 70 K and 185 K, respectively, consistent with our previous report.[8] For both K-under-doped and K-optimal-doped samples, Sb and P dopings steadily reduce T_C (Fig. 2(c)). The Curie–Weiss law, $(\chi + \chi_0)^{-1} = (T - \theta)/C$, where χ_0 is the temperature-independent term, has been employed to fit the magnetic data above their T_C. In Fig. 2(c), the obtained paramagnetic temperatures (θ) share the same alteration tendency with T_C for varying Sb- and P-doping levels. Meanwhile, coercivity field H_C and saturation moment M_S show some nonlinear relationship upon doping, particularly in K-optimal-doped $(Ba_{0.7}K_{0.3})(Zn_{0.85}Mn_{0.15})_2(As_{1-y}Pn_y)_2$ (Pn = Sb and P; $y = 0.1$ and 0.2). In Fig 2(d), we subtract the small H-linear component in the field-dependent magnetization loops ($M(H)$), which is presumably due to remaining paramagnetic spins and/or field-induced polarization,[6] to obtain the saturation moment at 2 K. H_C and M_S of 10% Sb are almost identical with those of $(Ba_{0.7}K_{0.3})(Zn_{0.85}Mn_{0.15})_2As_2$, even though the former's T_C is significantly lower than that of the latter. For the P-doped samples, H_C of 10% P is close to that of $(Ba_{0.7}K_{0.3})(Zn_{0.85}Mn_{0.15})_2As_2$, but its M_S is only half of the latter. With higher P level, both H_C and M_S are apparently reduced.

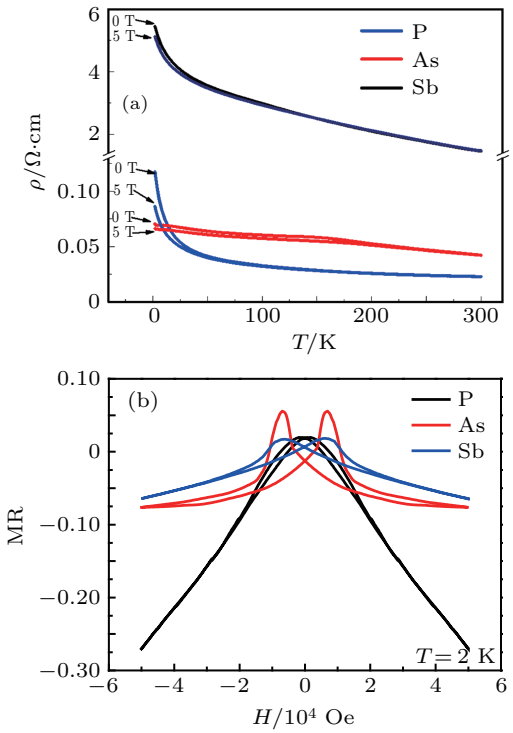

Fig. 3. (a) $(Ba_{0.7}K_{0.3})(Zn_{0.85}Mn_{0.15})_2(As_{1-y}Pn_y)_2$ (Pn = Sb and P; $y = 0.1$) samples' temperature dependent resistivity. (b) Field dependent resistivity of the samples in panel (a) at 5 K.

Figure 3(a) shows the temperature dependence of resistivity, $\rho(T)$, under $H = 0$ T and 5 T for $(Ba_{0.7}K_{0.3})(Zn_{0.85}Mn_{0.15})_2(As_{0.9}Pn_{0.1})_2$ with Pn = Sb, As, and P. For all the three samples, the resistivity increases with decreasing temperature, indicating a semiconducting behavior. In the entire temperature range, the resistivity of the Sb-doped sample is much higher than that of $(Ba_{0.7}K_{0.3})(Zn_{0.85}Mn_{0.15})_2As_2$. In contrast, the resistivity of the P-doped sample is lower than that of $(Ba_{0.7}K_{0.3})(Zn_{0.85}Mn_{0.15})_2As_2$ in most range of temperature. The tendency of resistivity changing with chemical pressure is consistent with our previous physical pressure studies which exhibited pressure induced semiconductor–metal transition in BZA.[8,10] In this work, (As,P) substitution compresses the cell volume, acting as a positive chemical pressure to increase the conductivity of $(Ba_{0.7}K_{0.3})(Zn_{0.85}Mn_{0.15})_2As_2$. In contrary, (As, Sb) substitution, which extends the cell volume, produces a negative chemical pressure and thus decreases the conductivity.

All three samples show negative magnetoresistance (MR) at low temperature regions. As shown in Fig. 3(b), the hystereses (i.e., H_C) observed from the $\rho(H)$ curves of $(Ba_{0.7}K_{0.3})(Zn_{0.85}Mn_{0.15})_2As_2$ and the Sb-doped sample are consistent with the $M(H)$ loops, while H_C of the P-doped one on $\rho(H)$ is somewhat smaller than that of the corresponding magnetic loop. MR_{2K} (MR defined as $(\rho_H - \rho)/\rho$) of $(Ba_{0.7}K_{0.3})(Zn_{0.85}Mn_{0.15})_2As_2$ is about -7% at $H = 5$ T, consistent with the previous report.[8,9] In many ferromagnetic materials, negative magnetoresistance results from the reduction of spin-dependent scattering by aligning the spins in the applied field. Within this scenario, compared to $(Ba_{0.7}K_{0.3})(Zn_{0.85}Mn_{0.15})_2As_2$, the decrease of MR in the Sb-doped sample is reasonable as the Sb-doped one has weaker ferromagnetic ordering. Unexpectedly, the P-doped sample shows much larger MR than $(Ba_{0.7}K_{0.3})(Zn_{0.85}Mn_{0.15})_2As_2$, even T_C of the former sample is smaller than that of the latter. Magnetoresistance effect is one of the most attractive functions of spintronic materials or devices. This modification on MR significantly extends the potential application of BZA.

In DMS, ferromagnetic ordering is mediated by carriers. Thus Hall effect was measured to probe possible change upon Sb- or P- doping. Figure 4 shows the Hall resistivity versus field ($\rho_H(H)$) for $(Ba_{0.7}K_{0.3})(Zn_{0.85}Mn_{0.15})_2As_2$ at 2 K and $(Ba_{0.7}K_{0.3})(Zn_{0.85}Mn_{0.15})_2(As_{0.9}Pn_{0.1})_2$ (Pn = Sb, As, and P) at 2 K, 50 K, and 100 K. The results demonstrate hole as the major carrier for all the three samples. At 2 K, anomalous Hall effect dominates the low field region for each sample. The shape of $\rho_H(H)$ loops is consistent with $M(H)$ loops at 2 K for the three samples, because the anomalous Hall part

is proportional to magnetization according to the phenomenological expression of the Hall resistivity, $\rho_{xy} = R_0 H + R_s M$, where R_0 is the ordinary Hall coefficient, R_s is the anomalous Hall coefficient, and M is the magnetization. With increasing temperature, the anomalous Hall part significantly decreases due to the weakened magnetization. Hole concentrations (n_p) calculated with the data in the high field region are tabulated in Table 1. Considering interference from remaining anomalous Hall part even in the high field region, we argue that n_p from Hall resistivity of 100 K is closer to the authentic value than that form the low-temperature. The n_p does not decrease but even slightly increases by Sb- and P-doping. Thus, the cause of the considerable reduction of T_C with Sb- and P-doping is still an open question for future studies.

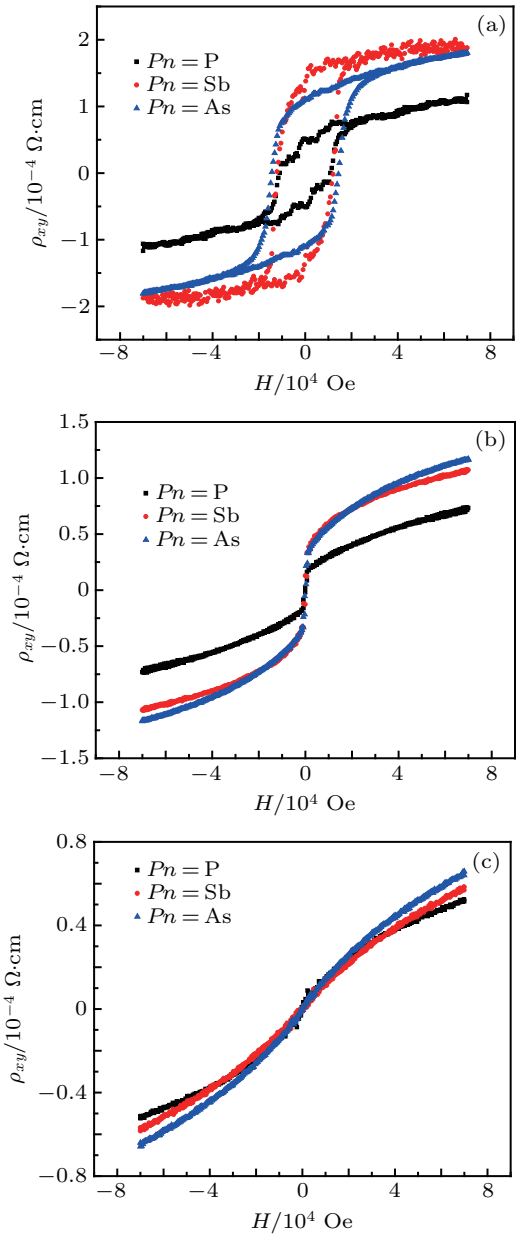

Fig. 4. $(Ba_{0.7}K_{0.3})(Zn_{0.85}Mn_{0.15})_2(As_{1-y}Pn_y)_2$ (Pn = Sb, As, and P; $y = 0.1$) samples' field dependent Hall resistivity at (a) 2 K, (b) 50 K, and (c) 100 K.

Table 1. The hole concentrations (in units of 10^{20} cm^{-3}) of $(Ba_{0.7}K_{0.3})(Zn_{0.85}Mn_{0.15})_2(As_{1-y}Pn_y)_2$ for $y = 0.1$.

Temperature/K	Pn = Sb	Pn = P	Pn = As
2	1.3	1.0	1.1
50	1.2	1.3	0.9
100	1.0	1.5	1.0

4. Conclusion and perspectives

Studies of external pressure-effects on BZA revealed suppression of Curie temperature upon compression. Iso-valent substitution of Sb or P into As in BZA to produce chemical pressure is an attractive attempt to tune the magnetic properties because previous studies on physical pressure-effects on BZA have revealed the suppression of Curie temperature upon compression. Although lattice extension does not increase T_C as expected, the change of resistivity with modification of cell volume has been reproduced. Nevertheless, the large MR effect induced by P-doping offers a new boulevard to improve magnetoelectric properties for spintronic materials.

Acknowledgment

Authors are grateful for the discussion with Maekawa S.

References

[1] Zutic I, Fabian J and Das Sarma S 2004 *Rev. Mod. Phys.* **76** 323
[2] Jungwirth T, Wunderlich J, Novák V, Olejník K, Gallagher B L, Campion R P, Edmonds K W, Rushforth A W, Ferguson A J and Němec P 2014 *Rev. Mod. Phys.* **86** 855
[3] Erwin S C and Žutić I 2004 *Nat. Mater.* **3** 410
[4] Ohno H 1998 *Science* **281** 951
[5] Chen L, Yang X, Yang F, Zhao J, Misuraca J, Xiong P and von Molnar S 2011 *Nano Lett.* **11** 2584
[6] Ohno H, Chiba D, Matsukura F, Omiya T, Abe E, Dietl T, Ohno Y and Ohtani K 2000 *Nature* **408** 944
[7] Deng Z, Jin C Q, Liu Q Q, *et al.* 2011 *Nat. Commun.* **2** 422
[8] Zhao K, Deng Z, Wang X C, *et al.* 2013 *Nat. Commun.* **4** 1442
[9] Zhao K, Chen B J, Zhao G Q, Yuan Z, Liu Q Q, Deng Z, Zhu J L and Jin C Q 2014 *Chin. Science Bulletin* **59** 2524
[10] Glasbrenner J K, Žutić I and Mazin I I 2014 *Phys. Rev. B* **90** 140403
[11] Sun F, Li N N, Chen B J, Jia Y T, Zhang L J, Li W M, Zhao G Q, Xing L Y, Fabbris G, Wang Y G, Deng Z, Uemura Y J, Mao H K, Haskel D, Yang W G and Jin C Q 2016 *Phys. Rev. B* **93** 224403
[12] Sun F, Zhao G Q, Escanhoela Jr C A, Chen B J, Kou R H, Wang Y G, Xiao, Y M Chow P, Mao H K, Haskel D, Yang W G and Jin C Q 2017 *Phys. Rev. B* **95** 094412
[13] Zhao G Q, Li Z, Sun F, Yuan Z, Chen B J, Yu S, Peng Y, Deng Z, Wang X C and Jin C Q 2018 *J. Phys.: Condens. Matter* **30** 254001
[14] Sun F, Xu C, Yu S, Chen B J, Zhao G Q, Deng Z, Wang Y G and Jin C Q 2017 *Chin. Phys. Lett.* **34** 067501
[15] Zhao G Q, Lin C J, Deng Z, Gu G X, Yu S, Wang X C, Gong Z Z, Uemera Y J and Li Y Q, Jin C Q 2017 *Sci. Reports* **7** 14473
[16] Wang R, Huang Z X, Zhao G Q, Yu S, Deng Z, Jin C Q, Jia Q J, Chen Y, Yang T Y, Jiang X M and Cao L X 2017 *AIP Adv.* **7** 045017
[17] Suzuki H, Zhao G Q, Zhao K, Chen B J, Horio M, Koshiishi K, Xu J, Kobayashi M, Minohara M, Sakai E, Horiba K, Kumigashira H, Gu B, Maekawa S, Uemura Y J, Jin C Q and Fujimori A 2015 *Phys. Rev. B* **92** 235120
[18] Frandsen B A, Gong Z, Terban M W, Banerjee S, Chen B J, Jin C Q, Feygenson M, Uemura Y J and Billinge S J L 2016 *Phys. Rev. B* **94** 094102
[19] Surmach M A, Chen B J, Deng Z, Jin C Q, Glasbrenner J K, Mazin I I, Ivanov A and Inosov D S 2018 *Phys. Rev. B* **97** 104418

[20] Gu G, Zhao G, Lin C, Li Y Q, Jin C Q and Xiang G 2018 *Appl. Phys. Lett.* **112** 032402
[21] Deng Z, Zhao K, Gu B, Han W, Zhu J L, Wang X C, Li X, Liu Q Q, Yu R C, Goko T, Frandsen B, Liu L, Zhang J S, Wang Y Y, Ning F L, Maekawa S, Uemura Y J and Jin C Q 2013 *Phys. Rev. B* **88** 081203
[22] Chen B J, Zhao K, Deng Z, Han W, Zhu J L, Wang X C, Liu Q Q, Frandsen B, Liu L, Cheung S, Ning F L, Munsie T J S, Medina T, Luke G M, Carlo J P, Munevar J, Uemura Y J and Jin C Q 2014 *Phys. Rev. B* **90** 155202
[23] Zhao K, Chen B J, Deng Z, *et al.* 2014 *J. Appl. Phys.* **116** 163906
[24] Han W, Zhao K, Wang X C, Liu Q Q, Ning F L, Deng Z, Liu L, Zhu J L, Ding C, Man H Y and Jin C Q 2013 *Sci. Chin. Phys. Mech. Astron.* **56** 2026
[25] Man H, Guo S, Sui Y, Guo Y, Chen B, Wang H, Ding C and Ning F L 2015 *Sci. Rep.* **5** 15507
[26] Ding C, Man H, Qin C, *et al.* 2013 *Phys. Rev. B* **88** 041102
[27] Chen B J, Deng Z, Wang X C, Feng S M, Yuan Z, Zhang S J, Liu Q Q and Jin C Q 2016 *Chin. Phys. B* **25** 077503
[28] Suzuki H, Zhao K, Shibata G, Takahashi Y, Sakamoto S, Yoshimatsu K, Chen B J, Kumigashira H, Chang F H, Lin H J, Huang D J, Chen C T, Gu B, Maekawa S, Uemura Y J, Jin C Q and Fujimori A 2015 *Phys. Rev. B* **91** 140401(R)
[29] Hirohata A, Sukegawa H, Yanagihara H, Zutic I, Seki T, Mizukami S and Swaminathan R 2015 *IEEE Trans. Magn.* **51** 0800511
[30] Zutic I and Zhou T 2018 *Sci. Chin.-Phys. Mech. & Astron.* **61** 067031